PREPRINT UCRL- 81575

Lawrence Livermore Laboratory

PRELIMINARY ZONAL MODEL ANALYSIS OF THE CLIMATIC CHANGE RESULTING FROM INCREASED ATMOSPHERIC CARBON DIOXIDE

Gerald L. Potter

November 1978

This paper was prepared for US/USSR Symposium of the Effects of Carbon Dioxide on Climate, October 10-21, 1978, Dushanbe, USSR.

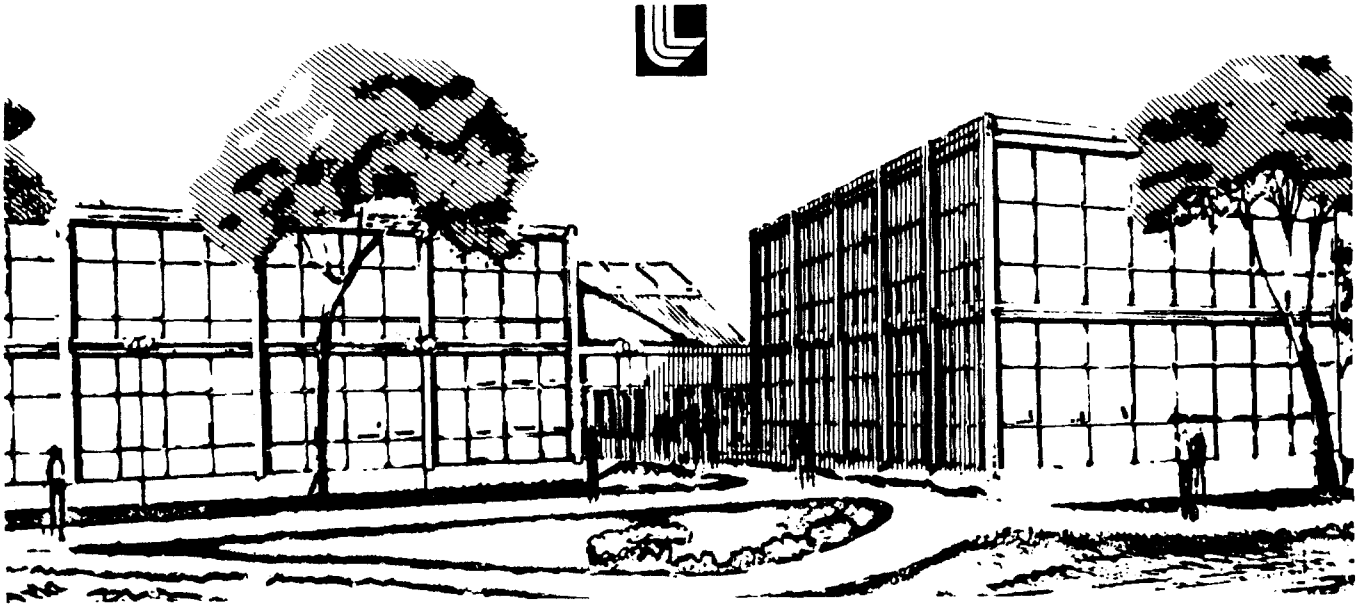

UCRL-81575

PRELIMINARY ZONAL MODEL ANALYSIS OF THE CLIMATIC CHANGE RESULTING FROM INCREASED ATMOSPHERIC CARBON DIOXIDE

Gerald L. Potter

Lawrence Livermore Laboratory, University of California,
Livermore, CA 94550

November 1978

INTRODUCTION

The increase in atmospheric carbon dioxide expected in the next few decades may result in a general increase in global surface temperatures. It is the purpose of this presentation to demonstrate how a two-dimensional zonal atmospheric model can be used to test the possible atmospheric response to various carbon dioxide concentrations. The response of a more complex three-dimensional general circulation model is well documented (Manabe and Wetherald, 1975) but to date, no experiments have been attempted with a comprehensive two-dimensional model. I present only the preliminary results that have provided a basis for future improvement of the model and better understanding of the feedback mechanisms that prevail given different atmospheric carbon dioxide concentrations.

MODEL DESCRIPTION

The two-dimensional zonal atmospheric model developed at the Lawrence Livermore Laboratory uses the primitive conservation equations and presently computes prognostic variables at nine vertical levels and at 10 degree intervals of latitude (see Luther and MacCracken (1974), MacCracken (1968), MacCracken, (1975) and MacCracken and Luther (1974)). The surface at each latitude is divided proportionally into land (of various types and elevations) and ocean (open or partial ice cover). The fractional representation allows a somewhat realistic treatment of the surface energy balances but without the spatial coherence of a continental structure. The surface treatment allows fluxes of sensible heat and moisture to be calculated from gradients of temperature and water vapor, respectively, the surface wind velocity and the appropriate bulk transfer coefficients.

Clouds are calculated at four levels and are a function of relative humidity and calibrated with data from London (1957). Convection is a function of cloud overlap, vertical lapse rate, and moisture content. The mechanism relates the lapse rate adjustment (convective intensity) to the departure from the local moist adiabatic lapse rate rather than forcing the model to a prescribed fixed lapse rate.

The land surface is divided into as many as 10 layers of variable depth to facilitate matching the thermal inertia to diurnal and seasonal forcing. The number of snow and ice layers depends on the total accumulated depth. The ocean is treated as an isothermal layer of prescribed

depth corresponding to that of the thermocline. The ocean temperature depends on the surface energy balance and a prescribed meridional ocean heat flux. The model also calculates sea ice depth and extent depending on the temperature and energy balance of the ocean layer at that latitude.

MODEL PERFORMANCE

Although the annual average version is used in this experiment, it is important that we validate the seasonally varying model against other models and observations to better understand model sensitivity. The seasonal version and the annual average version are similar with the exception that the latter has a latitudinally-dependent fixed annual average solar flux and a reduced ocean depth to permit more rapid convergence to a near-equilibrium state.

Figures 1-4 demonstrate some aspects of the model's performance for the month of January using the seasonal version (Potter et al. (1978) gives more complete performance data). Figure 1 shows the zonally averaged cloud cover as compared with observations and various other models.* The divergence from the observations in the high northern latitudes is believed to be due to difficulties in the relative humidity

*In all comparisons, GCM's are labeled with **, radiative convective models with *, the LLL zonal model with ZAM2 and observations by a reference alone.

fields. Figure 2 shows how the zonal precipitation compares with two general circulation models and observations. The reason for the exaggerated precipitation (Fig. 2) and evaporation (Figure 3) in the tropical latitudes may be a result of a too active Hadley cell.

In terms of radiation, Fig. 4 shows the absorbed solar radiation at the earth's surface. This implies that the surface albedo is properly treated and that the general influence of cloud cover in terms of shortwave radiation is reasonable compared to other model calculations and observations.

THE CO_2 EXPERIMENTS

In order to decrease the computer time requirements and to increase the number of model experiments undertaken for this presentation, we used the annual average version of the model. The computational time required for the model is approximately 10 minutes per model month on a class IV computer. Starting from initial conditions similar to observed zonally averaged temperature, moisture and momentum fields, the model was integrated with respect to time for 200 days. The carbon dioxide perturbations (1/2 times present CO_2, 2 times present CO_2 and 4 times present CO_2) and the control run were then integrated for an additional 200 days. Near-equilibrium was assumed to be reached when the net storage of heat at the earth's surface approached zero. In addition, the total planetary heat change attained at the near-equilibrium state is

near 10^{-4} ly min^{-1}. As suggested by Manabe and Wetherald (1975) this value is negligible for all practical purposes.

TEMPERATURE

The latitude-height difference in temperature between the perturbed atmosphere and the control case are shown in Figs. 5, 6 and 7 for 1/2 x CO_2, 2 x CO_2 and 4 x CO_2 respectively. The reduced CO_2 concentration in the 1/2 x CO_2 case allows more heat to be lost to space thus cooling the troposphere. The stratospheric warming results from the decreased emission from the stratospheric CO_2 to space. Since the absorption of solar radiation in the stratosphere by ozone does not change with changing CO_2, the reduction in CO_2 requires an increase in temperature for longwave radiation to balance solar absorption in the stratosphere. The identical processes are operating with a reversed sign in the increased CO_2 cases (2 x CO_2 and 4 x CO_2). That is, the increased CO_2 cases, the stratosphere cools and the troposphere warms.

Figures 8, 9 and 10 show the surface temperature difference for the three cases (Figs. 5, 6 and 7 extend down to only the lowest prognostic level which, in most cases, is 1000 mb). The surface temperatures display the exaggerated polar response to increased atmospheric CO_2 but for apparently different reasons than those reported by Manabe and Wetherald (1975). This response results from insufficient poleward eddy transport of heat and water vapor for all experiments. This in turn,

produces too steep a poleward temperature gradient and extremely cold polar temperatures. In the case of increased atmospheric temperatures from CO_2 the polar warming is confined to the shallow atmospheric layer near the surface where only a slight increase in radiant energy results in an amplified warming in this thin layer below the inversion. The amplified polar temperature response results almost entirely from this change associated with the inversion while the ice-albedo feedback mechanism was essentially ineffective in amplifying temperatures in these model runs. Another feature of the model that may limit sensitivity to changing CO_2 are the snow and sea-ice depths (and extent) which are calculated explicitly. Snow continuously accumulates in the annual average version which additionally limits sensitivity to warming global temperatures.

At some stage, probably upon insertion of more realistic eddy transport, we expect the model to exhibit some features of the ice-albedo feedback. With some exceptions (e.g., surface temperature change at $70^{\circ}N$ for the 4 x CO_2 case), the response was similar to that calculated by Manabe and Wetherald (1975). The Northern Hemisphere average surface temperature increase for 2 x CO_2 was 2.3 K and for 4 x CO_2, 3.7 K. The Southern Hemisphere, and thus global changes as well, were smaller.

HYDROLOGY

Figure 11 shows the total precipitation for the control and each of the perturbations. As CO_2 increased so did global precipitation. The

globally averaged precipitation for the control case was 0.269 cm day^{-1}; for 2 x CO_2, 0.285 cm day^{-1} (6% increase); for 4 x CO_2, 0.294 cm day^{-1} (9% increase); and for 1/2 x CO_2, .259 cm day^{-1} (4% decrease). The increased tropospheric downward longwave radiation from CO_2 increased the surface energy available for evaporation, which in turn further increased the downward longwave radiation from the atmosphere.

ALBEDO

As mentioned earlier, the snow and ice cover did not change appreciably in the CO_2 experiments. Yet because of the moisture dependence of the surface albedo (wet soil is darker than dry soil) the Northern Hemisphere surface albedo (a_n) decreased as the CO_2 content increased. For 1/2 x CO_2, a_n = 22.8%; control a_n = 22.4%; 2 x CO_2, a_n = 22.2%; and 4 x CO_2, a_n = 19.1%. The 4 x CO_2 case displayed some increase in snow extent at 60°N resulting in a further drop in surface albedo. The Southern Hemisphere displayed no significant changes in surface albedo, which in large part was due to the complete lack of sea ice in the high southern latitudes. Given the ice-free situation in the Southern Hemisphere, the warming from CO_2 and water vapor lacked the magnification of temperatures due to the ice-albedo feedback mechanism.

HEAT BALANCE

The area mean heat balance for various concentrations of CO_2 is shown in Fig. 12. The net longwave radiation at the surface decreased with higher CO_2 concentrations. For the 1/2 x CO_2 case the net radiation at the surface (incoming shortwave minus outgoing longwave) decreased 4.9% while for the 2 x CO_2 case the net radiation increased 4.2% and for the 4 x CO_2 case it increased 6.3%. This can be attributed to the increased solar absorption (lower surface albedo) and the reduced loss of longwave radiation (because of increased atmospheric counterradiation from CO_2 and water vapor). Because of the warmer surface temperatures, the Bowen ratio (sensible heat/latent heat) decreased since evaporation is more effective in removing heat from the surface than turbulent heat.

Planetary albedo (Fig. 13) compares quite favorably with observations compiled by Rashke et al. (1973). Recent data from Ellis (personal communication) suggest that the values from Rashke et al. (1973) are quite low in the high northern latitudes and that the zonal model results are quite similar to observations. Figures 14, 15 and 16 show the change in planetary albedo resulting from increased CO_2 (perturbed minus control). Increasing CO_2 reduced the planetary albedo at almost all latitudes. Figure 16 (difference in planetary albedo for the 4 x CO_2 case) shows the influence of the reduction in snow cover on one land surface type fraction at $60^{o}N$. The areas of strongest response were at $30^{o}S$ and $40^{o}S$ where cloud cover increased caused the planetary albedo to also increase.

Only those Southern Hemispheric changes in planetary albedo noted above appear to have exhibited a significant effect on surface temperatures. This indicates that the model is possibly too sensitive to change in cloud cover since the decrease in shortwave radiation from increased clouds should be nearly balanced by the increased downward longwave radiation from the clouds (Cess, 1976). Ideally, the experiments should be repeated with fixed cloud cover to more fully document the cloud sensitivity.

POLEWARD TRANSPORT OF ENERGY

Because of the reduction of poleward temperature gradient in the Northern Hemisphere, the meridional transport of total atmospheric energy ($c_pT + L_r + \kappa\omega T/P$) decreased with increased CO_2. (Fig. 17) Here c_pT represents sensible heat, L_r represents latent heat and $\kappa\omega T/P$ is the transport occurring due to conversion from potential to kinetic energy. Conversely, the poleward transport in the Southern Hemisphere increased (southward transport is negative). This paradox can be at least partially explained by the relative insensitivity of the Antarctic temperatures to changes in atmospheric CO_2. In these numerical experiments, the model computed no changes in the Antarctic sea-ice distribution and therefore, with the general global warming from increased CO_2, the gradient increased in the Southern Hemisphere resulting in increased southward transport. This again may not be realistic since one

would expect sea-ice to form near Antarctica for at least part of the year, which would initiate ice-albedo feedback.

CONCLUSIONS

This study was a preliminary numerical experiment to test the climatic effect of various atmospheric CO_2 concentrations with a zonal atmospheric model with feedback mechanisms. The main results of this analysis may be summarized as follows:

1. The increased CO_2 warmed the troposphere and reduced the intensity of the polar surface inversions which in turn magnified the temperature response with latitude. This response was similar to the Manabe and Wetherald (1975) computation but different mechanisms were largely responsible. In the case of the zonal model, polar temperatures were very cold, and the warming associated with the increased CO_2 and water vapor only partially compensated for the intense sub-freezing temperatures. Consequently, no snow or ice melted but the surface temperatures increased.
2. The magnitude of the stratospheric temperature difference increased with altitude as CO_2 concentrations were increased.
3. Precipitation, evaporation and the total atmospheric water content increased with increasing CO_2 concentrations. The Bowen ratio (H/LE) decreased with increasing CO_2.

ACKNOWLEDGMENTS

I would like to thank Drs. H. W. Ellsaesser and M. C. MacCracken for their valuable comments and suggestions. I also thank Mr. Ken Hill for his assistance in performing these calculations. This work was performed under the auspices of the U. S. Department of Energy by Lawrence Livermore Laboratory under contract No. W-7405-Eng-48.

REFERENCES

Budyko, M. I., 1973, Atlas of the Heat Balance of the Earth, Gidormeteorizdat, Moscow, 69 pp.

Cess, R. D., 1976, "Climate Change: An Appraisal of Atmospheric Feedback Mechanisms Employing Zonal Climatology," J. Atmos. Sci., 33, No. 10, pp. 1831-1843.

ETAC (Environmental Technical Application Center), 1971, U. S. Air Force, Northern Hemisphere Cloud Cover, Project 6168, Washington, DC.

Holloway, J. L., Jr. and S. Manabe, 1971, "Simulation of Climate by a Global General Circulation Model, 1. Hydrologic Cycle and Heat Balance," Monthly Weather Review, 99, pp. 335-369.

Kahle, A. B. and F. Haurwitz, 1973, The Radiation and Heat Budget of the Mintz-Arakawa Model: January, The Rand Corporation, R-1318-ARPA.

Katayama, A., 1967, "On the Radiation Budget of the Troposphere over the Northern Hemisphere (II), Hemispheric Distribution," J. Meteor. Soc. Japan, Ser. 2, 45, pp. 1-25.

London, J., 1957, A Study of the Atmospheric Heat Balance, Final Report, Contract AF 19 (122) - 165, Research Division, College of Engineering, New York University, 99 p.

Luther, F. M. and M. C. MacCracken, 1974, "Initial Validation Studies for ZAM2 Radiation and Large Scale Eddy Transport Mechanisms," Third Conference on CIAP, Feb. 26-March 1, 1974, Report No. DOT-TSC-OST-74-15, pp. 437-449.

MacCracken, M. C., 1968, Ice Age Theory by Computer Simulation, Ph.D. Thesis, University of California, Davis, 193 pp.

MacCracken, M. C., 1975, "Climate Model Results of Stratospheric Perturbations," in Proceedings of the Fourth Conference on CIAP, Dept. of Transportation, DOT-TSC-OST-75-38, pp. 183-194.

MacCracken, M. C. and F. M. Luther, 1974, "Climate Studies Using a Zonal Atmospheric Model," in Proceedings - International Conference on Structure, Composition and General Circulation of the Upper and Lower Atmosphere and Possible Anthropogenic Perturbations, Melbourne, Australia, January 14-25, 1974, W. L. Godson ed., V. II, pp. 1107-1128, Atmospheric Environment Service, Ontario, Canada.

Manabe, S. and R. T. Wetherald, 1975, "The Effects of Doubling the CO_2 Concentration on the Climate of a General Circulation Model," J. Atmos. Sci., 32, pp. 3-15.

Potter, G. L., H. W. Ellsaesser, M. C. MacCracken and F. M. Luther, 1978, "Atmospheric Statistical Dynamic Models. Model Performance: The Lawrence Livermore Laboratory Zonal Atmospheric Model," in Proceedings of the GARP WMO-ICSU Joint Organizing Committee, A Review of Climate Models: Performance, Intercomparison and Sensitivity Studies, held in Washington, DC April 1978.

Rashke, E., T. H. Vonder Haar, W. R. Bandeen, and M. Pasternak, 1973, "The Annual Radiation Balance of the Earth-Atmosphere System During 1969-1970 from Nimbus 3 Measurements," J. Atmospheric Sci., 30, pp. 341-364.

Sasamore, T., J. London, and D. V. Hoyt, 1972, "Radiation Budget of the Southern Hemisphere," Chapter 2, in Meteorology of the Southern Hemisphere, Meteor. Monographs, 13 35.

Schutz, C., and W. L. Gates, 1972, Global Climatic Data for Surface, 800 mb, 400 mb: January, The Rand Corporation, R-915-ARPA.

Schutz, C., and W. L. Gates, 1972, Supplemental Global Climatic Data: January, The Rand Corporation, R-915/1-ARPA.

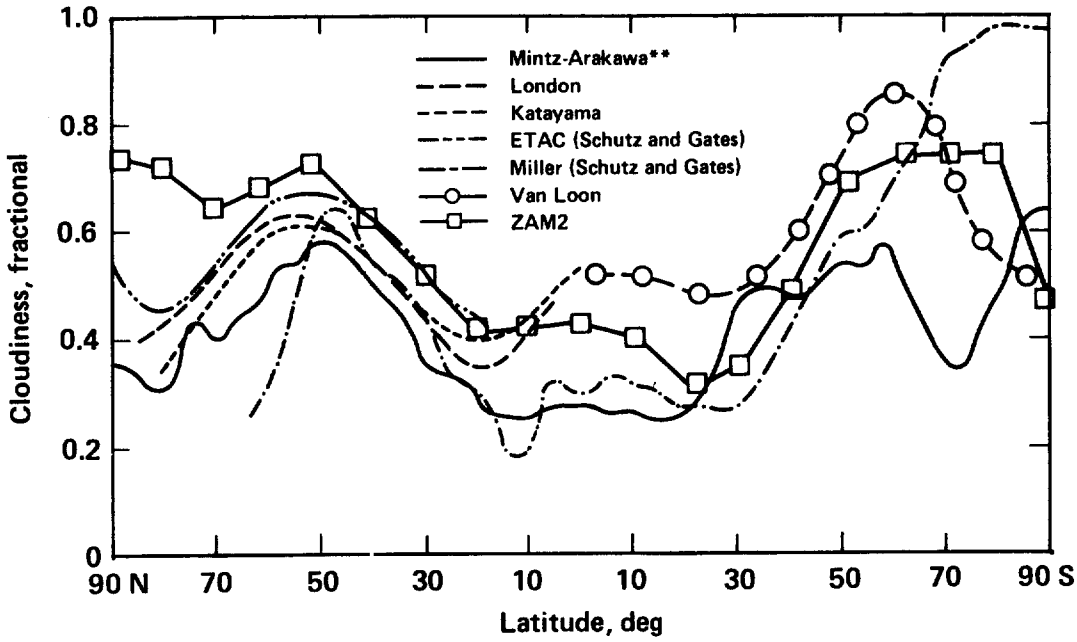

Figure 1. The zonally averaged total cloud cover, from Kahle and Haurwitz (1973).

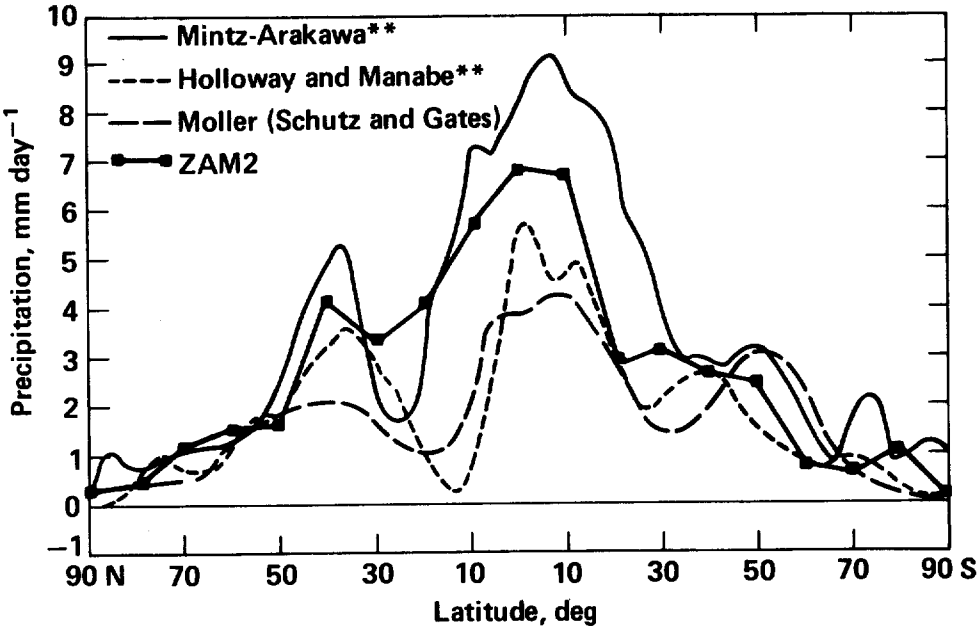

Figure 2. The zonally averaged precipitation, from Kahle and Haurwitz (1973).

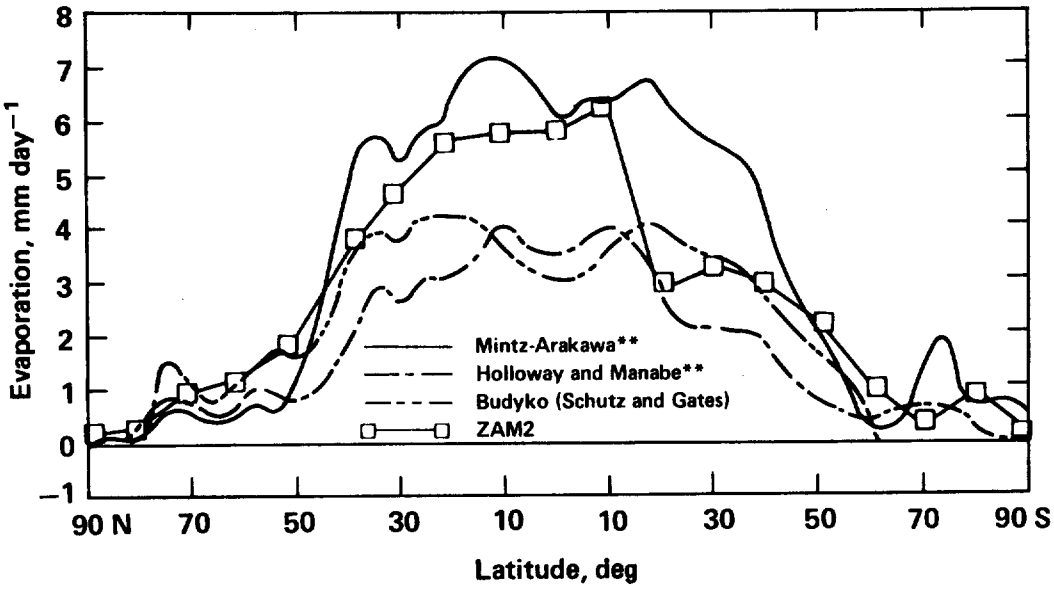

Figure 3. The zonally averaged evaporation, from Kahle and Haurwitz (1973).

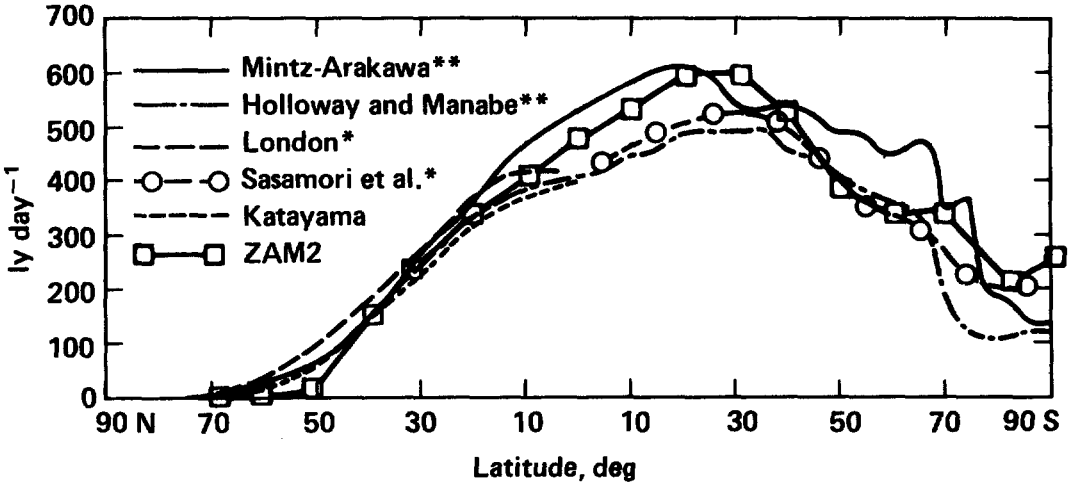

Figure 4. The zonally averaged solar radiation absorbed by the earth's surface, from Kahle and Haurwitz (1973).

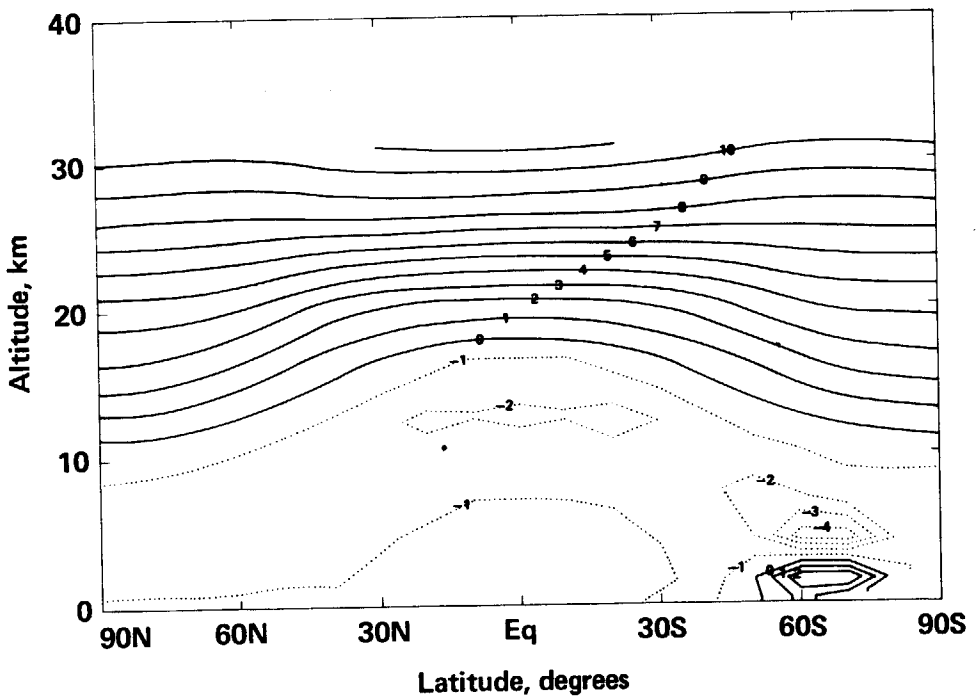

Figure 5. Temperature difference (1/2 x CO_2 - control) contour interval = 1.00°K.

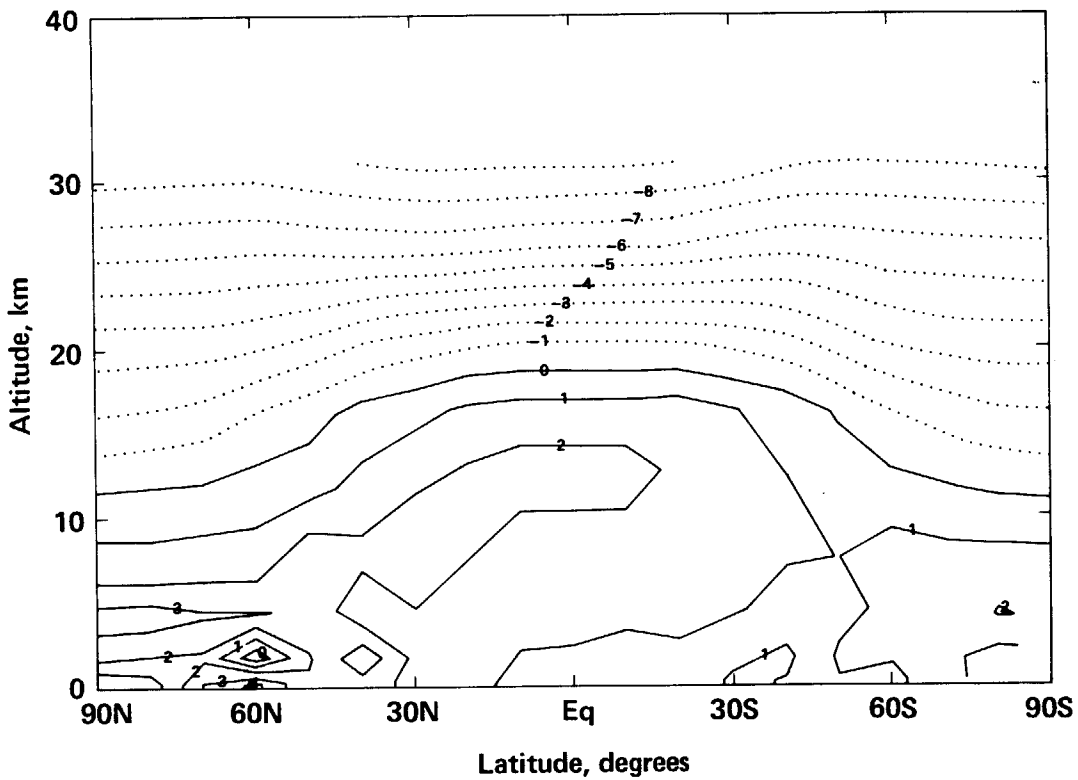

Figure 6. Temperature difference (2 x CO_2 - control)
contour interval = 1.00°K.

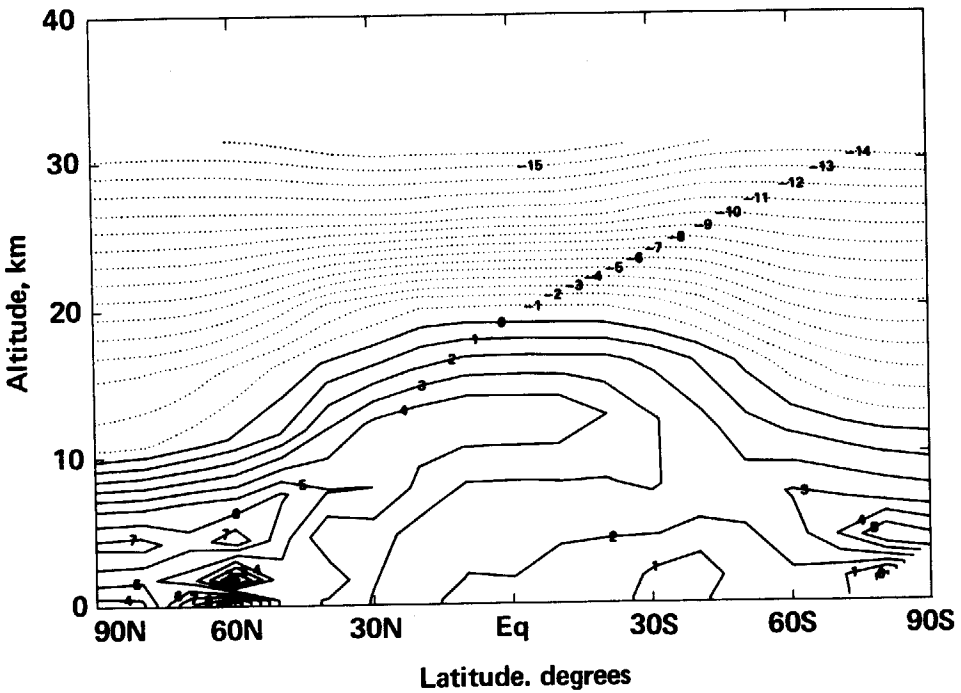

Figure 7. Temperature difference (4 x CO_2 - control)
contour interval = 1.00°K.

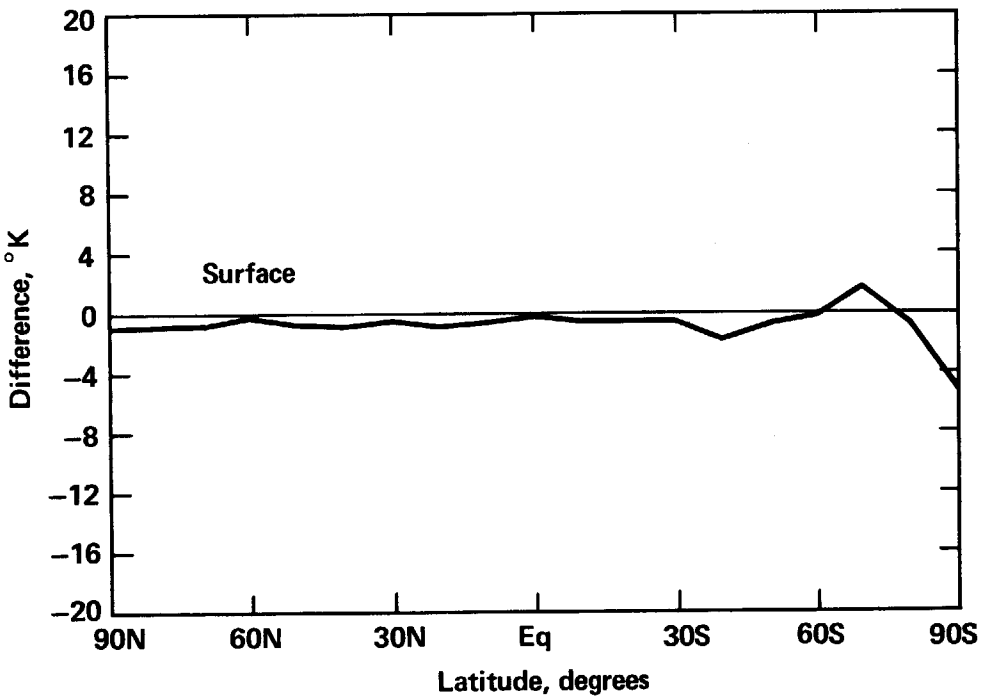

Figure 8. Temperature difference (1/2 CO_2 - control).

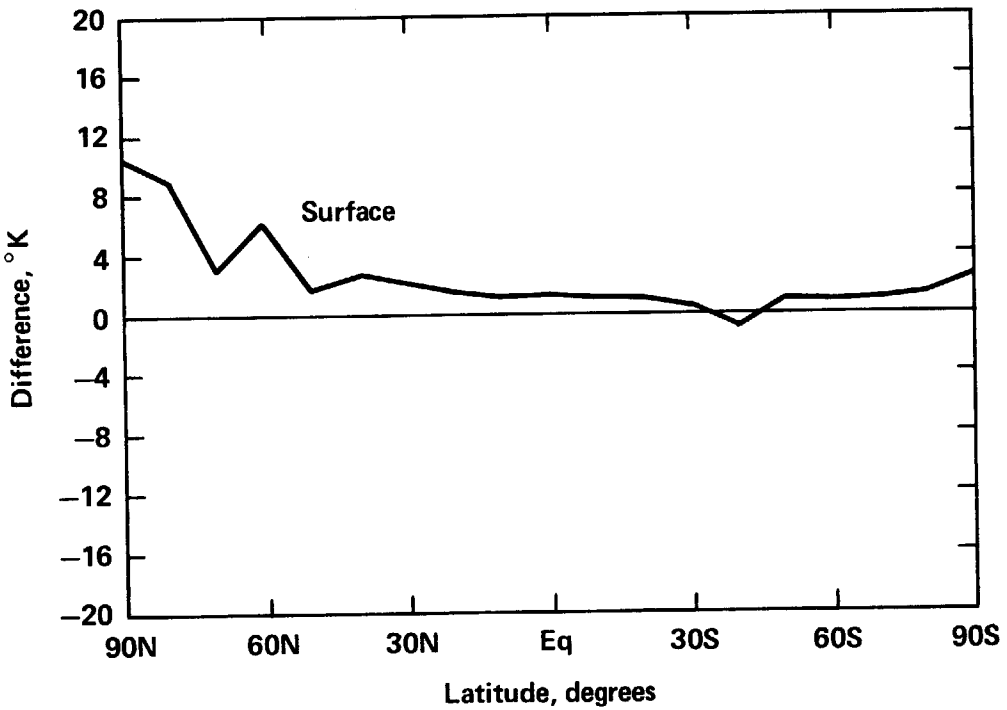

Figure 9. Temperature difference (2 x CO_2 - control).

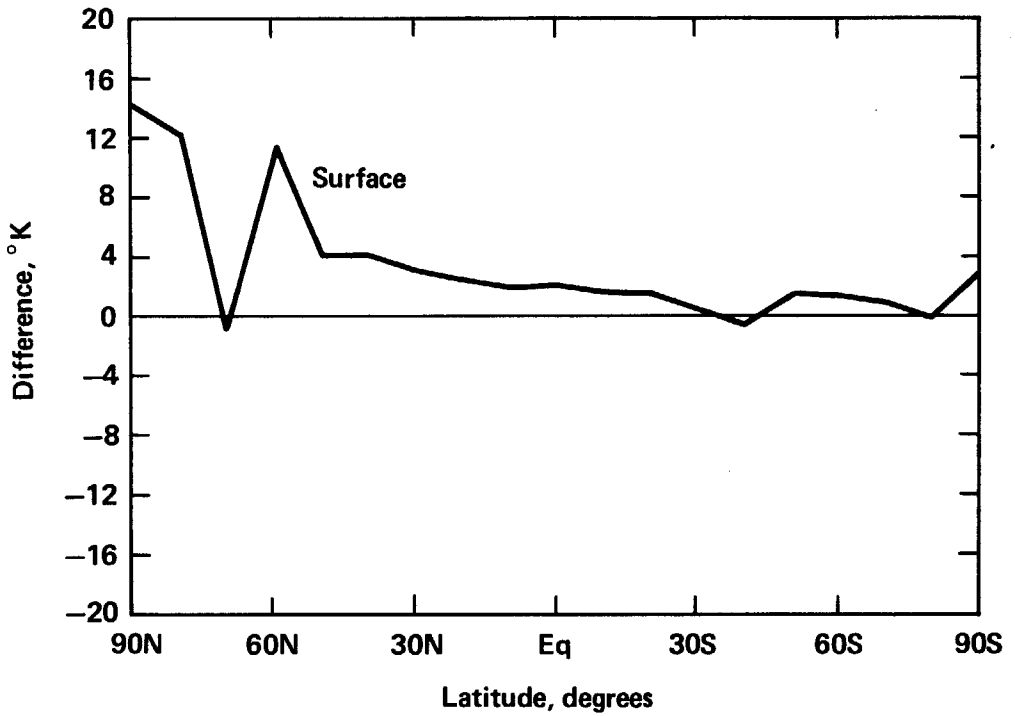

Figure 10. Temperature difference (4 x CO_2 - control).

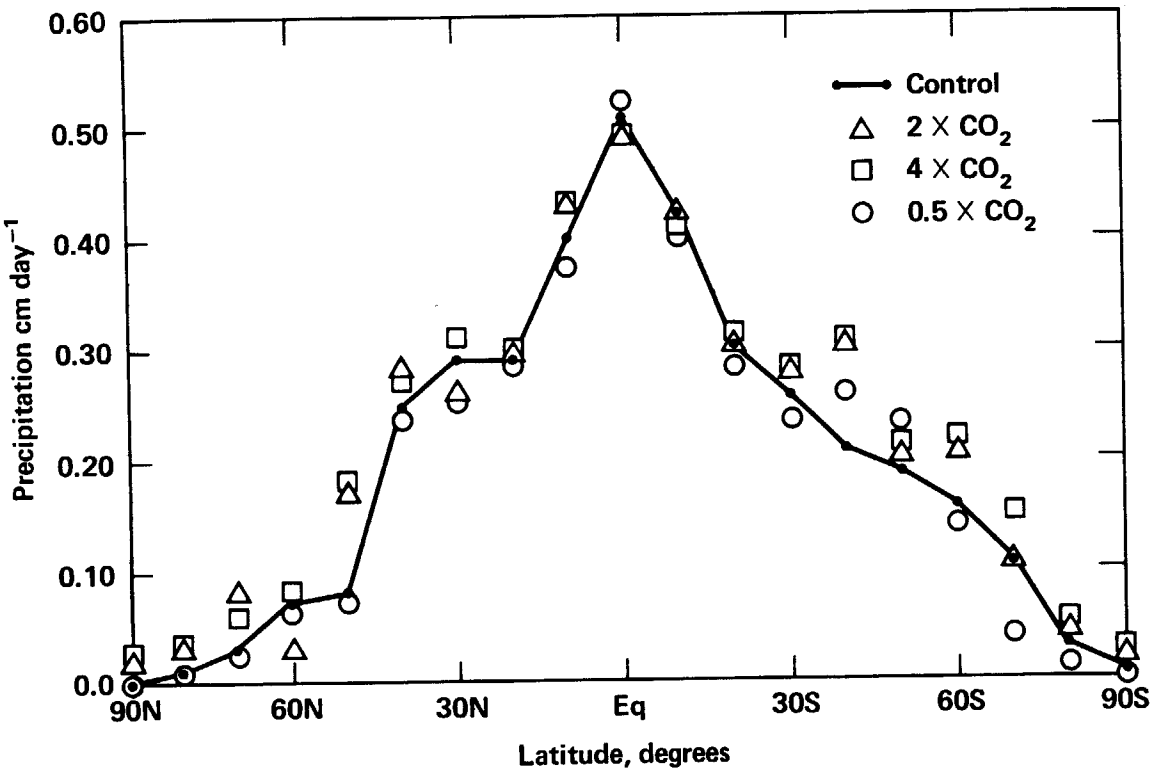

Figure 11. Total precipitation cm day^{-1}.

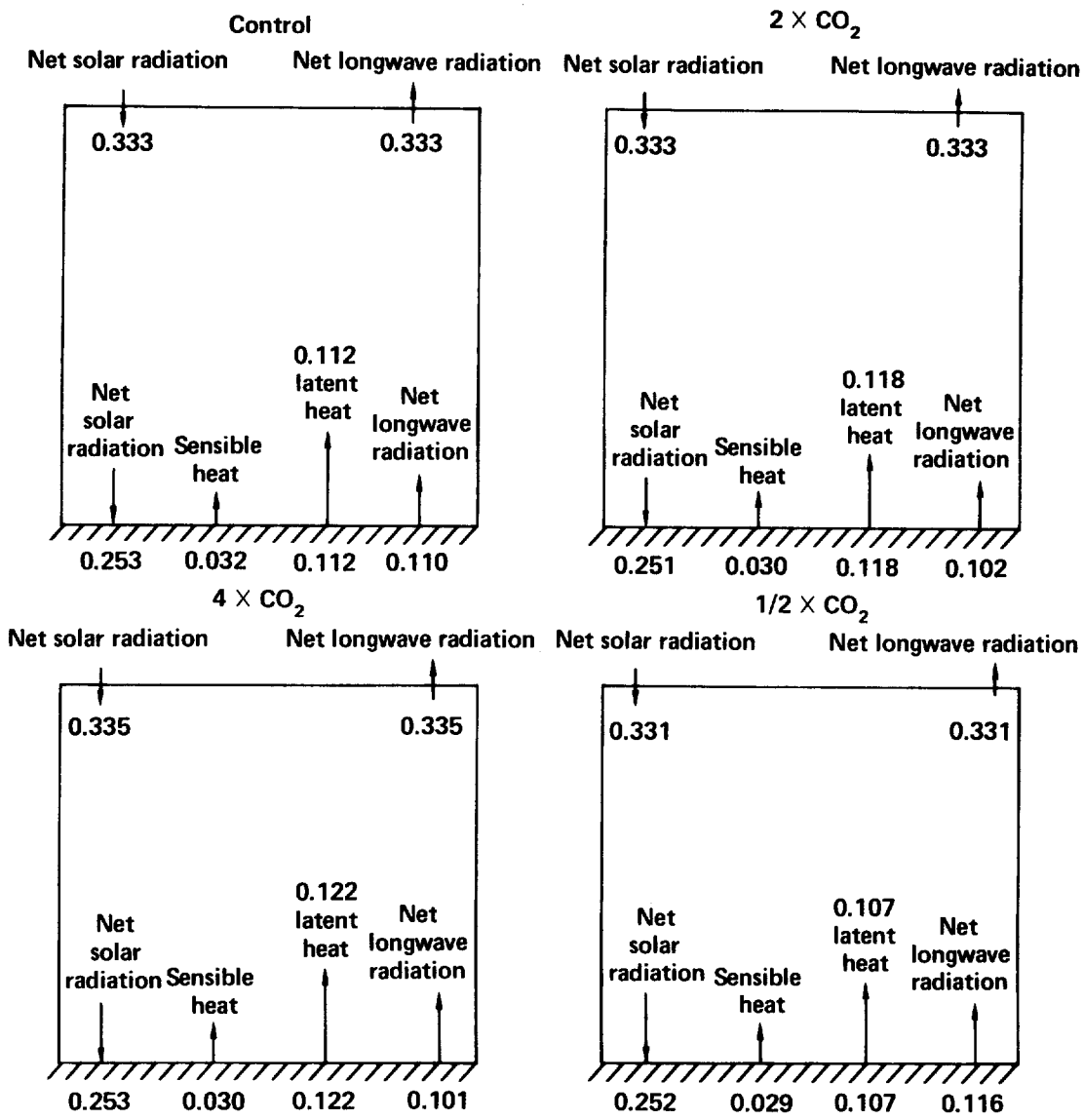

Figure 12. Area mean heat balance (ly min^{-1}).

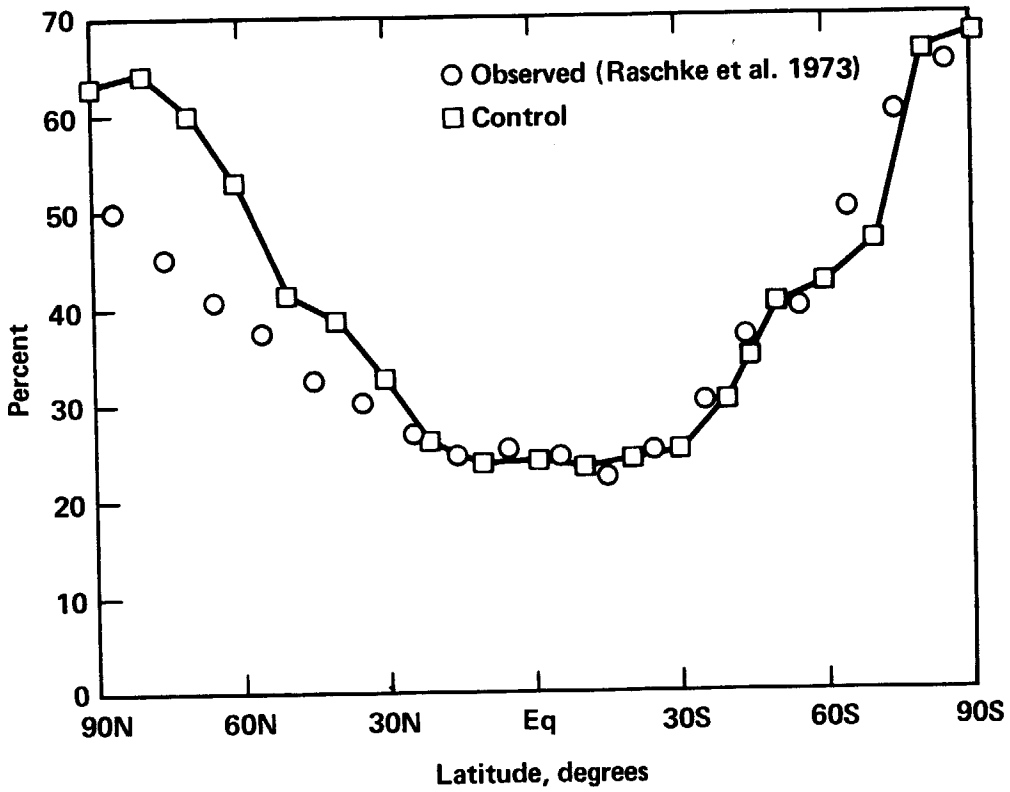

Figure 13. Planetary albedo.

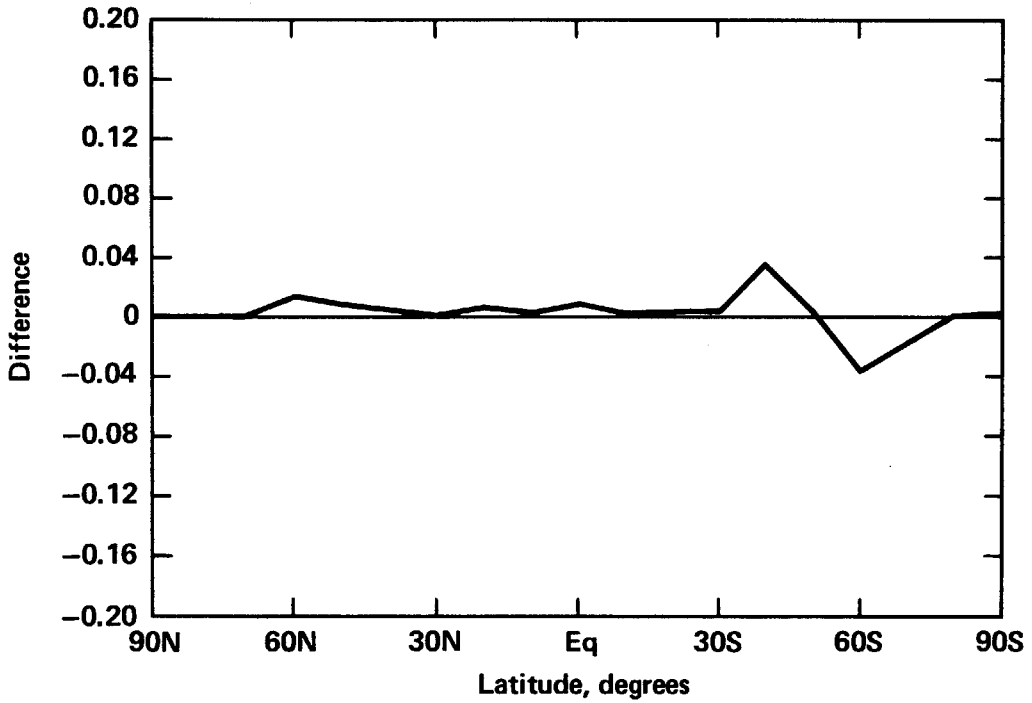

Figure 14. Difference in planetary albedo (1/2 x CO_2 - control).

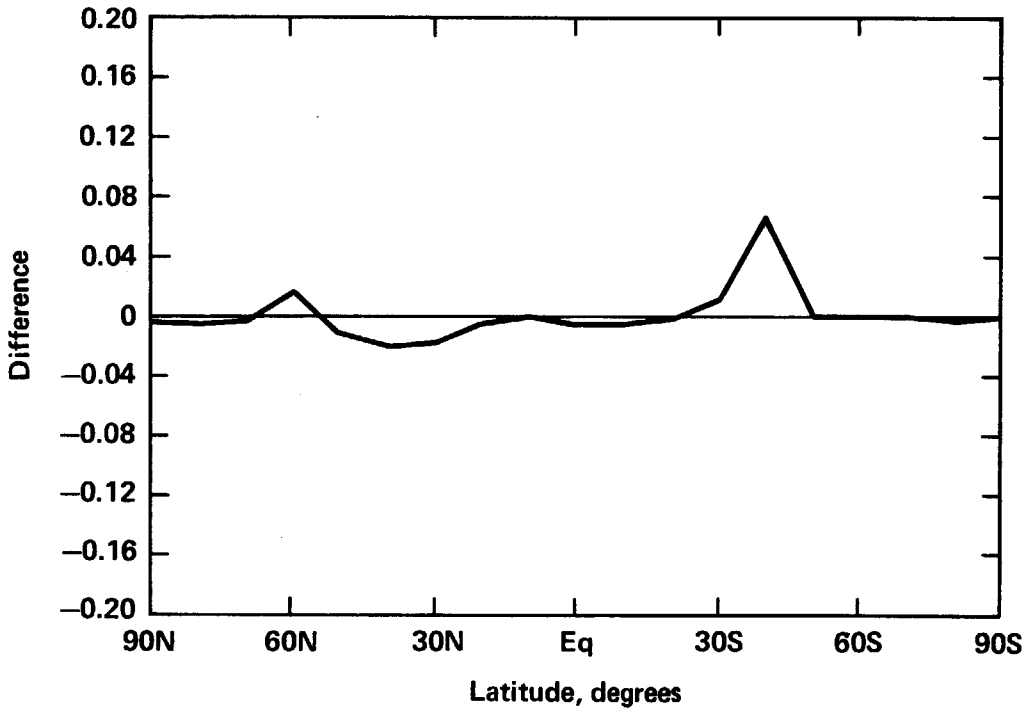

Figure 15. Difference in planetary albedo (2 x CO_2 - control).

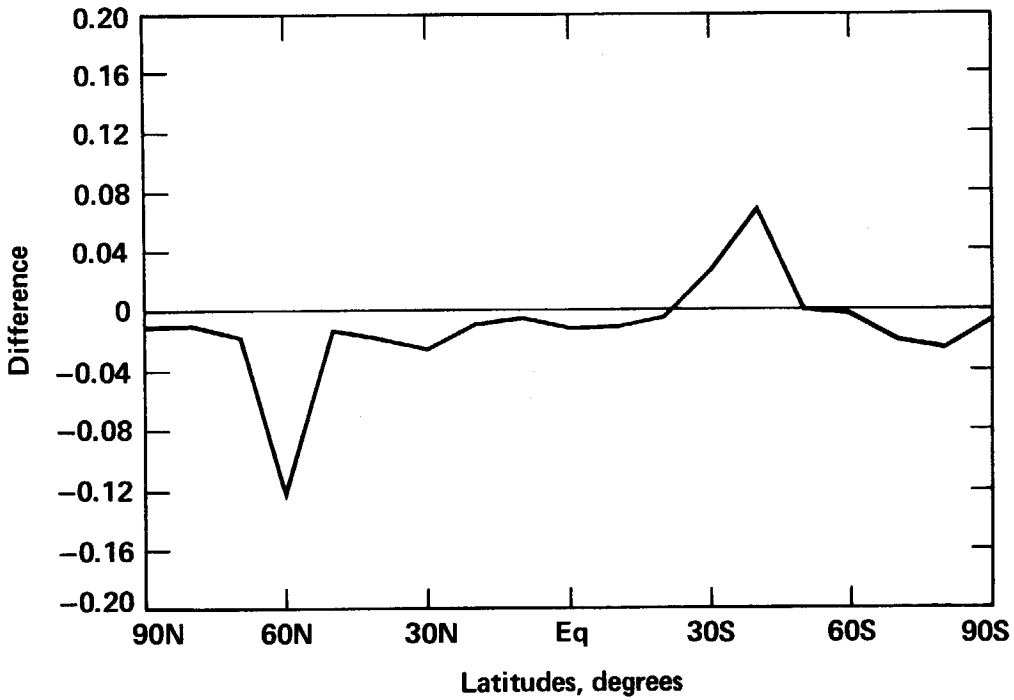

Figure 16. Difference in planetary albedo ($4 \times CO_2$ - control).

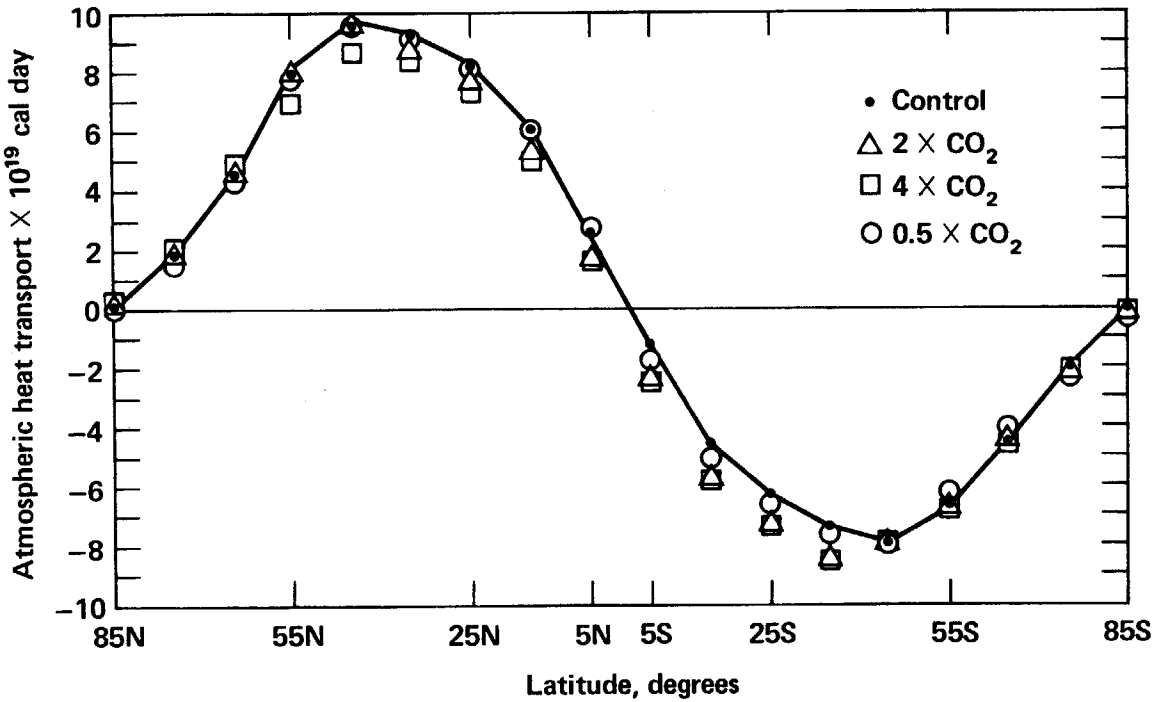

Figure 17. Poleward transport of atmospheric energy.